

**Impact of Data Quality and Surface-to-Column Representativeness on the
PM_{2.5}/Satellite AOD Relationship for the Continental United States**

**Travis D. Toth¹, Jianglong Zhang¹, James R. Campbell², Edward J. Hyer², Jeffrey S.
Reid², Yingxi Shi¹, and Douglas L. Westphal²**

¹Dept. of Atmospheric Sciences, University of North Dakota, Grand Forks, ND, USA
²Aerosol and Radiation Sciences Section, Marine Meteorology Division, Naval Research
Laboratory, Monterey, CA, USA

Submitted to:

Atmospheric Chemistry and Physics

15 October 2013

¹ Corresponding Author Contact: Dr. Jianglong Zhang, c/o Department of Atmospheric Sciences, 4149

E-mail: jzhang@atmos.und.edu

ABSTRACT

Satellite-derived aerosol optical depth (AOD) observations have been used to estimate particulate matter less than 2.5 μm ($\text{PM}_{2.5}$). However, such a relationship could be affected by the representativeness of satellite-derived AOD to surface aerosol particle mass concentration and satellite AOD data quality. Using purely measurement-based methods, we have explored the impacts of data quality and representativeness on the AOD inferred $\text{PM}_{2.5}$ /AOD relationship for the Continental United States (CONUS). This is done through temporally and spatially collocated datasets of $\text{PM}_{2.5}$ and AOD retrievals from Aqua/Terra Moderate Resolution Imaging Spectroradiometer (MODIS), Multi-angle Imaging Spectroradiometer (MISR), and Cloud-Aerosol Lidar with Orthogonal Polarization (CALIOP). These analyses show that improving data quality of satellite AOD, such as done with data assimilation-grade retrievals, increases their correlation with $\text{PM}_{2.5}$. However, overall correlation is relatively low across the CONUS. Also, integrated extinction observed within the 500 m above ground level (a.g.l.), as measured by CALIOP, is not well representative of the total column AOD. Surface aerosol in the Eastern CONUS is better correlated than in the Western CONUS. The best correlation values are found for estimated dry mass CALIOP extinction at 200-300 m a.g.l. and $\text{PM}_{2.5}$, but additional work is needed to address the ability of using actively sensed AOD as a proxy for $\text{PM}_{2.5}$ concentrations.

1 **1.0 Introduction**

2
3 Particulate matter (PM), especially suspended particles and solution droplets with
4 diameters smaller than 2.5 μm ($\text{PM}_{2.5}$), contributes greatly to regional air pollution and
5 can pose a threat to human health [e.g., Schwartz and Neas, 2000; Pope et al., 2002].
6 Traditionally, the United States (U.S.) Environmental Protection Agency (EPA) has
7 monitored surface-based $\text{PM}_{2.5}$ concentrations using either a gravimetric-based method at
8 ground stations with 24-hour filter samplers or hourly Tapered Element Oscillating
9 Microbalance (TEOM) and beta gauge samplers. [Federal Register, 1997]. A number of
10 studies have attempted estimates of surface-based $\text{PM}_{2.5}$ concentrations using satellite-
11 retrieved aerosol optical depth (AOD) data [e.g., Hutchison, 2003; Wang and Christopher,
12 2003; Engel-Cox et al., 2004; Kumar et al., 2007; Liu et al., 2007; Hoff and Christopher,
13 2009]. The advantages of estimating surface-based $\text{PM}_{2.5}$ concentrations using satellite-
14 derived AOD data are obvious, as satellites, including both polar orbiting and
15 geostationary satellites, typically provide a much larger spatial coverage than what can be
16 inferred from ground stations over a broad surface footprint. However, data is limited to
17 daylight cloud free conditions with once per day collection by polar orbiters [Diner et al.,
18 1998; Remer et al., 2005] or multiple images in morning or afternoon from geostationary
19 satellites [Zhang et al., 2001; Prados et al., 2007].

20 Previous research efforts have focused on algorithm development for solving PM
21 proxies based on AOD. For example, Chu et al., [2003] compare PM_{10} concentrations
22 with surface AOD measurements from the Aerosol Robotic Network (AERONET) in
23 northern Italy and highlight the potential of using Moderate Resolution Imaging
24 Spectroradiometer [MODIS; Remer et al., 2005] AOD as an estimate for PM_{10}

25 concentration. Several studies have focused on correlating satellite AOD observations
26 and $PM_{2.5}$ concentrations [e.g., Wang and Christopher, 2003; Liu et al., 2004], and
27 advances have been made improving correlation between the two by considering other
28 meteorological and environmental parameters, such as the surface mixed-layer height
29 [Engel-Cox et al., 2006; Gupta et al., 2006] and relative humidity [Shinozuka et al., 2007;
30 Van Donkelaar et al., 2010]. Simulated vertical structure from chemical transport
31 models [e.g., Van Donkelaar et al., 2006; 2010] has also been used to help improve the
32 $PM_{2.5}$ /satellite AOD relationship.

33 There are important issues, however, that need be considered when applying
34 satellite-based observations in general, much less as a proxy for $PM_{2.5}$ estimates. First,
35 uncertainties exist in satellite-retrieved AOD values due to issues such as cloud
36 contamination, inaccurate optical models used in the retrieval process and heterogeneous
37 surface boundary conditions [e.g., Zhang and Reid, 2006; Shi et al., 2011a; Toth et al.,
38 2013]. Even today, convergence has not yet been reached for retrieved AOD values
39 found among the most widely used satellite aerosol products, such as the Dark
40 Target/DeepBlue MODIS and Multi-angle Imaging Spectroradiometer [MISR; Diner et
41 al., 1998; Kahn et al., 2010] aerosol products [e.g., Shi et al., 2011b]. Any estimate of
42 $PM_{2.5}$ derived from satellite AOD data cannot be more accurate than the AOD data
43 themselves. Thus, relationships between AOD and $PM_{2.5}$ are likely to be highly sensor
44 product specific. Second, AOD derived from passive sensors is a column-integrated
45 value, and $PM_{2.5}$ concentration is a surface measurement. Under conditions where
46 aerosol particles are concentrated primarily within the surface/boundary layer, AOD is
47 presumably a likelier proxy for $PM_{2.5}$ concentration. Conversely, in conditions where

48 aerosol plumes are transported above the boundary layer, AOD will likely prove a weaker
49 one. Finally, AOD is a column-integrated sum of total ambient particle extinction,
50 whereas PM_{2.5} is measured with respect to dried particle ingested for analysis by
51 corresponding instruments. Thus, hygroscopicity and mass extinction efficiency
52 corrections are further required to accurately characterize any relationship present
53 between the two parameters.

54 While some studies have attempted to use chemical transport models and ground-
55 based lidars to investigate a relationship between aerosol particle structure, column-
56 integrated AOD and surface-based PM_{2.5} [Liu et al., 2004; Van Donkelaar et al., 2006;
57 Boyouk et al., 2010; Hyer and Chew, 2010], a measurement-based analysis using the
58 Cloud-Aerosol Lidar with Orthogonal Polarization [CALIOP; Winker et al., 2007; Hunt
59 et al., 2009] would allow for such a study over relatively-broad spatial and temporal
60 scales, for which more tenable proxies between AOD and PM_{2.5} may be realized and thus
61 applied on more representative scales. Range-resolved information collected with
62 CALIOP provides the critical perspective for relating the depth and vertical extent of
63 aerosol particle presence to both surface-based PM_{2.5} measurements and passive retrievals
64 of column-integrated AOD.

65 This paper differs from past research efforts in several aspects. For one, the impact
66 of passive satellite AOD data quality on the PM_{2.5}/satellite AOD relationship has yet to
67 be investigated. Secondly, while other studies have considered the aerosol vertical
68 distribution during estimation of PM_{2.5} from satellite AOD retrievals, this has not been
69 examined over large spatial and temporal domains. Lastly, to the best of our knowledge,
70 near-surface aerosol extinction from CALIOP has never been evaluated as a potential

71 proxy for surface PM_{2.5} concentrations. Therefore, through the use of MODIS, MISR,
72 and CALIOP observations, the following research questions are considered:

- 73 1. How does the quality of passive satellite AOD retrievals impact the PM_{2.5}/AOD
74 relationship?
- 75 2. Based on CALIOP data, how representative are surface-based measurements to
76 aerosol particle presence within the full column?
- 77 3. Can near surface observations from CALIOP be used as a better proxy for PM_{2.5}
78 concentration?

79 The paper has been designed to discuss each component sequentially, thus building off
80 the previous step. In Sec. 2 of this paper, we describe the various satellite and surface-
81 based datasets used. In Sec. 3, the PM_{2.5}/AOD relationship is first examined at an hourly
82 timescale, followed by a daily analysis in which we explore the impact of AOD quality
83 on this relationship. In Sec. 4, we investigate the representativeness of satellite-derived
84 surface aerosol concentration to that of the entire column, and how well surface AOD
85 correlates with total column AOD. Lastly in Sec. 5, we provide results comparing
86 surface-based PM_{2.5} and CALIOP aerosol extinction near the lower bounds of the satellite
87 profile to investigate the potential use of CALIOP data for air quality applications.

88

89 **2.0 Datasets**

90

91 **2.1 MODIS, MISR, and CALIOP Data**

92

93 Aboard both the NASA Aqua and Terra satellites, MODIS is a spectroradiometer
94 with 36 channels (0.41 to 15 μm), seven of which (0.47 to 2.13 μm) are applied
95 operationally for the retrieval of aerosol particle optical properties. The Dark Target

96 Level 2 products created from these retrievals are reported at a spatial resolution of 10 x
97 10 km², with over-land uncertainties of $0.05 \pm 0.15 \times \text{AOD}$ [Remer et al., 2005]. This
98 study utilizes the Corrected_Optical_Depth_Land (0.550 μm) parameter of Dark Target
99 Level 2 Collection 5.1 retrievals from Aqua (MYD04_L2) and Terra (MOD04) MODIS
100 (2008-2009, operational), with quality assurance (QA) limiting the analysis to only those
101 retrievals with Quality_Assurance_Land parameter flags of “very good”. Although the
102 DeepBlue (DB) MODIS aerosol products also provide aerosol retrievals over land, the
103 Collection 5.1 Aqua/Terra DB MODIS aerosol products are not available for the study
104 period and are thus not included in the study.

105 MISR, aboard the Terra satellite, is a unique spectroradiometer, able to collect
106 observations at nine different viewing angles, providing a means for studying aerosol
107 particle size and shape [Diner et al., 1998]. MISR features four spectral bands, located at
108 0.446, 0.558, 0.672, and 0.867 μm . Different from the Dark Target MODIS aerosol
109 products, the MISR aerosol product also includes AOD retrievals over bright surfaces
110 such as desert regions. Kahn et al. [2005] suggested that 70% of MISR AOD data are
111 within 0.05 (or $20\% \times \text{AOD}$) of sun-photometer measured AOD values. This study
112 utilizes the same two years (2008-2009) of AOD derived from Version 22 MISR
113 retrievals (0.558 μm), flagged through QA screening as “successful”.

114 CALIOP is a multi-wavelength (0.532 and 1.064 μm) polarization lidar flown
115 aboard the Cloud-Aerosol Lidar and Infrared Pathfinder Satellite Observations
116 (CALIPSO) platform within the NASA “A-Train” constellation [e.g., Stephens et al.,
117 2002]. To gain an understanding of aerosol particle distribution over the U.S. for 2008-
118 2009, this study utilizes the Version 3.01 CALIOP Level 2 5 km Aerosol Profile

119 (L2_05kmAProf) [Winker et al., 2007; Winker et al., 2012] product. The Version 3.01
120 Level 2 Vertical Feature Mask (L2_VFM) product is also used to restrict the analysis to
121 those 5 km AOD and total extinction (at 0.532 μm) profile retrievals that are cloud-free,
122 in a manner consistent with that of Toth et al. [2013].

123

124 **2.2 Quality-Assured MODIS and MISR Subsets**

125

126 Existing uncertainties in passive satellite AOD retrievals, such as those for
127 MODIS and MISR, are optimally suppressed before being considered and applied for
128 data assimilation (DA) activities involving operational aerosol forecast models [e.g.,
129 Zhang et al., 2008]. Through rigid QA, reduced AOD uncertainties have been
130 characterized and DA-quality AOD datasets have been created for both over land [Hyer
131 et al., 2011] and over ocean MODIS DT products [Shi et al., 2011a], as well as the MISR
132 aerosol products [Shi et al., 2011b; 2012]. In this study, we use DA-quality MODIS and
133 MISR AOD products as control datasets for comparison with operational MODIS and
134 MISR products.

135 Available at 6-hourly $1^\circ \times 1^\circ$ resolution, DA-quality AOD data are converted to
136 daily averages and then compared with daily $\text{PM}_{2.5}$ concentrations. For comparison
137 purposes with the $\text{PM}_{2.5}$ data available (described further below), we have constructed
138 daily-averaged ‘Level 3’ AOD data using operational MODIS and MISR aerosol
139 products after applying first-order QA as described in Sec. 2.1. DA-quality MODIS
140 aerosol products are available from the Global Ocean Data Assimilation Experiment
141 (GODAE) server (<http://www.usgodae.org/>). However, no quality-assured hourly DA-

142 quality aerosol products are currently available, and no comparisons were therefore made
143 between the DA-quality products and hourly PM_{2.5} measurements.

144

145 **2.3 Surface PM_{2.5}**

146

147 The U.S. EPA has collected observations of surface-based PM since the passage
148 of the Clean Air Act in 1970 (<http://www.epa.gov/air/caa/>). In 1997, the EPA began
149 specifically monitoring PM_{2.5} concentrations [Federal Register, 2006]. The Federal
150 Reference Method (FRM), a filter-based method, is used to measure concentration over a
151 continuous 24-hr period. The filter is weighed before and after the sample collection
152 interval and PM_{2.5} mass concentration ($\mu\text{g}/\text{m}^3$) is calculated by dividing the total mass of
153 PM_{2.5} particles by the volume of air sampled [Federal Register, 1997]. Some EPA sites
154 also report hourly (continuous) PM_{2.5} measurements. For this study, two years (2008-
155 2009) of daily and hourly PM_{2.5} Local Conditions (EPA Parameter Code 88101) data
156 were used and obtained from the EPA Air Quality System (AQS).

157

158 **2.4 AERONET AOD**

159 AERONET is a worldwide ground-based network of sun photometers that
160 provides measurements of aerosol optical properties, and is currently used as the
161 benchmark for validation of satellite AOD retrievals. AERONET AOD is reported at
162 eight channels (0.34 to 1.64 μm), and has an uncertainty of 0.01 to 0.015 [Holben et al.
163 1998]. For the purposes of this study, AOD derived at 0.67 μm is used.

164

165 **3.0 How Does the Quality of Passive Satellite AOD Retrievals Impact their Linear** 166 **Correlation with Surface-Based PM_{2.5}?**

167
168 As a first step, linear correlations between passive satellite AOD retrievals and
169 $PM_{2.5}$ observations in the United States are derived. We investigate the impact of data
170 quality to the AOD/ $PM_{2.5}$ relationship through a daily analysis using both daily-averaged
171 operational and DA-Quality AOD datasets, as well as daily $PM_{2.5}$ data. No hourly DA-
172 quality AOD retrievals are currently available, and therefore the impact of data quality to
173 the AOD/ $PM_{2.5}$ correlations are not specifically characterized on this temporal scale. Still,
174 an hourly analysis is first considered, using only operational AOD data and hourly $PM_{2.5}$
175 data, for comparison purposes and for establishing a relevant context for the relationship
176 between AOD and $PM_{2.5}$.

177 Figure 1 depicts those $PM_{2.5}$ monitoring sites for the 2008-2009 period that reported
178 hourly (Fig. 1a) and daily-averaged (Fig. 1b) $PM_{2.5}$ observations. A total of 102 sites
179 reported hourly data, while 991 sites collected daily data (see figure caption for color
180 scheme). Note that some sites feature multiple instruments observing $PM_{2.5}$
181 concentration; one routine/primary, regular measurement and a secondary measurement
182 that is only available sporadically. Both types of $PM_{2.5}$ data are included for this analysis.

183

184 **3.1 Hourly Analysis**

185

186 For 2008-2009, the operational Level-2 AOD datasets are spatially and temporally
187 collocated with available $PM_{2.5}$ observations. After these AOD data are filtered through
188 basic QA screening (Sec. 2.1), each hourly $PM_{2.5}$ observation is matched with those
189 Level-2 AOD retrievals meeting the QA criteria and found within 40 km and 1 hr of the
190 $PM_{2.5}$ observation. All remaining AOD values are then averaged for a single comparison
191 with the $PM_{2.5}$ observation. We chose 40 km as the averaging range for the satellite data

192 after assuming a mean wind speed of 10 m/s influencing aerosol plumes transport
193 (approximately 40 km/hr). AOD autocorrelation at or exceeding 0.8 has been reported
194 for a distance of 40 km (on average) [Anderson et al., 2003; Zhang et al., 2011], making
195 this a reasonable constraint.

196 Table 1 summarizes the results of the hourly collocation of 40 km/1 hr average
197 MODIS/MISR AOD with corresponding ground-based PM_{2.5} measurements over the two
198 year study, including linear correlation coefficients and data counts for the contiguous
199 U.S. divided into its four respective time zones: Eastern (UTC-5), Central (UTC-6),
200 Mountain (UTC-7), and Pacific (UTC-8). Relatively low correlations are found for the
201 U.S., as a whole. However, a regional dependence of the relationship between the two
202 parameters is also apparent. The Eastern U.S. region exhibits higher correlation than
203 does the Pacific U.S. by a factor of nearly two (0.2 vs. 0.4). This is consistent with
204 several studies that have shown similar regional effects. For example, Hu [2009] reports
205 average PM_{2.5}/AOD correlations of 0.67 (Eastern U.S.) and 0.22 (Western U.S.), with
206 Engel-Cox et al. [2004] and Paciorek et al. [2008] reporting similar correlations of 0.6-
207 0.8 (Eastern U.S.) and 0.2-0.4 (Western U.S.). It has been suggested that this regional
208 variability in the PM_{2.5}/AOD relationship is due to differences in topography, surface
209 albedo, and boundary layer depth between the Eastern and Western U.S. [Engel-Cox et
210 al., 2006].

211 In Fig. 2, regional differences of PM_{2.5}/AOD correlation are also evident from
212 scatterplots for the Eastern (Figure 2a) and Pacific (Figure 2b) time zones, with greater
213 linearity observed in the Eastern U.S. compared to the west. Also, PM_{2.5} concentration
214 averages were computed for each 0.1 bin of AOD, and shown with respect to both Terra

215 MODIS and MISR. Note that although we have listed both Aqua and Terra MODIS in
216 Table 1, we show only the Terra MODIS/MISR analysis in Fig. 2 because of their
217 common satellite-observing platform. In general, a better correlation is found for the bin
218 averages, which is consistent with that reported by Gupta et al., [2006].

219 Seasonally, each of the hourly $PM_{2.5}$ /AOD correlations coefficients shown in
220 Table 1 are recomputed for December through May (Table 1; DJFMAM) and June
221 through November (Table 1; JJASON). There are fewer data points for DJFMAM than
222 JJASON (~68% decrease), enhanced by the absence of December 2007 in the dataset
223 (this month was not included in the analysis due to the lack of $PM_{2.5}$ Local Conditions
224 data, EPA Parameter Code 88101, before 2008). Overall, however, lower correlations
225 are found during this season compared with the annual mean. The opposite is thus true
226 for JJASON. Although not shown here, further analysis reveals that higher correlations
227 of JJASON may be due to a significant number of cases of relatively high $PM_{2.5}$ (greater
228 than $35 \mu\text{g}/\text{m}^3$) and high satellite AOD (greater than 0.3) that occur during this season,
229 relative to DJFMAM, which may positively influence the regression compared with
230 JJASON.

231

232 3.2 Daily Analysis

233

234 We next investigate how the relationship between AOD and $PM_{2.5}$ is affected by the
235 perceived data quality of the operational satellite AOD datasets, using only basic QA,
236 versus the DA-quality Level 3 AOD data. As discussed above, these latter data are
237 subject to more advanced screening, with filtering, correction, and spatial aggregation
238 applied. Each available daily ground-based $PM_{2.5}$ observation is matched with both the

239 operational and DA-quality AOD retrievals found within 1° latitude/longitude and the
240 day of the $PM_{2.5}$ observation. Results of the daily $1^\circ \times 1^\circ$ operational and DA-quality
241 MODIS/MISR AOD analyses are shown for the CONUS and each respective time zone
242 in Table 2.

243 Distinct increases are found for $PM_{2.5}$ /AOD correlation using the DA-quality
244 satellite AOD products versus the operational satellite AOD datasets (Table 2). For
245 example, $PM_{2.5}$ /AOD correlations for the CONUS increase by about 0.12 (Aqua MODIS),
246 0.16 (Terra MODIS), and 0.14 (MISR) from each respective operational to DA-quality
247 dataset. Note that data counts for each DA-quality AOD analysis decrease relative to
248 each corresponding operational AOD analysis, indicative of fewer available collocations
249 from the Level 3 AOD datasets from increased data rejection. We believe that such a
250 pronounced pattern reflects the influence of AOD retrieval quality from the passive
251 satellites on their relationship with surface-based $PM_{2.5}$ measurements.

252 Also shown in Table 2, the Eastern sample exhibits greater linearity (i.e.,
253 correlation) overall compared with the Western one. Figure 3 further illustrates the
254 regional variation in $PM_{2.5}$ /DA AOD correlation, through corresponding scatterplots for
255 the Eastern (Figure 3a) and Pacific (Figure 3b) time zones. As in Fig. 2, we only show
256 the Terra MODIS/MISR analysis because of their common platform. Also, averages of
257 $PM_{2.5}$ concentrations are shown for each 0.1 bin of DA TERRA and MISR AOD

258 The seasonality of the $PM_{2.5}$ /AOD relationship for the daily analysis is investigated
259 in Table 2. As encountered above for Table 1, there are fewer data points for DJFMAM
260 than JJASON (~32% decrease). Likewise, lower $PM_{2.5}$ /AOD correlations are found
261 during DJFMAM, and higher correlations are found from JJASON, as compared to the

262 mean annual results presented in Table 2. Again, this pattern may be due to a larger
263 number of high $PM_{2.5}$ (greater than $35 \mu\text{g}/\text{m}^3$) and high satellite AOD (greater than 0.3)
264 values that are found from JJASON, as compared to DJFMAM. However, a longer study
265 period is likely needed to more appropriately understand the seasonal dependence of the
266 $PM_{2.5}$ /AOD relationship.

267 Figure 4 consists of two maps depicting daily $PM_{2.5}$ sites used in this analysis, color-
268 coded with respect to $PM_{2.5}$ /AOD correlation coefficient. Figure 4a reflects the
269 $PM_{2.5}$ /daily operational Terra MODIS AOD relationship, with generally higher
270 correlations in the Eastern U.S. than the Pacific U.S. Figure 4b illustrates a clear increase
271 in $PM_{2.5}$ /AOD correlation for the daily DA Terra MODIS AOD analysis, with again still
272 higher correlations for the Eastern U.S. compared to those results found in the west.
273 Similar regional and operational-to-DA AOD patterns in the $PM_{2.5}$ /AOD relationship are
274 shown in Figure 5 for the operational MISR AOD (Figure 5a) and DA MISR AOD
275 (Figure 5b) daily analyses.

276 In order to strengthen the results obtained in the hourly and daily analyses, we apply
277 a common point filter to the data. Our common point filter refers to the requirement of
278 valid points from all four data sources (i.e., hourly/daily $PM_{2.5}$ and operational/DA AOD).
279 As such, for common $PM_{2.5}$ sites, correlations between hourly $PM_{2.5}$ and 40 km average
280 operational AOD, and daily $PM_{2.5}$ and $1^\circ \times 1^\circ$ average DA AOD, were computed (Table
281 3). Regional variations in the $PM_{2.5}$ /AOD relationship found here are similar to those in
282 earlier analyses presented in this paper, with higher correlations for the east than for the
283 west. Also, the correlations from the hourly analysis are generally higher than those from
284 the daily analysis, but with some dependency on region and satellite sensor. While this

285 common point study implies that operational AOD may be a better estimate of PM_{2.5} than
286 DA AOD, we note here that when only daily data are used (Table 2), there exists a
287 distinct improvement in PM_{2.5} estimation from the operational to DA AOD datasets.
288 Thus, it is reasonable to expect further improvement in the PM_{2.5}/passive satellite AOD
289 relationship through the use of hourly DA-quality AOD datasets. These data are
290 currently not readily available, however, so this topic is left for a future study.

291 As a final step for Section 3, we examine the hourly PM_{2.5}/AERONET AOD
292 relationship for the CONUS. AERONET AOD (0.67 μm) measurements found within
293 0.3° latitude/longitude and the hour of an hourly PM_{2.5} observation were first averaged,
294 and hourly PM_{2.5}/AERONET AOD correlations and data counts were then computed
295 (Table 4). Similar to the results from the PM_{2.5}/satellite AOD analyses, a higher
296 correlation is found for the Eastern Time zone (0.57) compared to the Pacific Time zone
297 (0.47). Also, the hourly PM_{2.5}/AERONET AOD correlations are generally higher than
298 those between hourly PM_{2.5}/satellite AOD (Table 1). These findings are not surprising,
299 as AERONET is considered the benchmark for validation of satellite AOD retrievals.

300

301 **4.0 How Representative is the Surface Layer Aerosol Particle Presence to the**

302 **Atmospheric Column?**

303 We have demonstrated that the quality of the AOD datasets investigated impacts
304 any linear correlation apparent with ground-based PM_{2.5} measurements. Next we explore
305 the representativeness of aerosol particle presence near the surface to that of the
306 atmospheric column. We use the CALIOP L2_05kmAProf product, featuring a vertical
307 resolution of 60 m for altitudes below 20.2 km above mean sea level (MSL). Using the

308 corresponding mean surface elevation reported with each profile, values of extinction
309 coefficient and AOD ($0.532 \mu\text{m}$) are re-gridded linearly at 100 m resolution vertically
310 from the surface (above ground level, or a.g.l.) to 8.2 km after a robust QA screening
311 procedure takes place. The details of this QA process are documented in past studies
312 [Kittaka et al., 2011; Campbell et al., 2012a; Winker et al., 2012; Toth et al., 2013]. Only
313 cloud-free profiles are considered.

314 Shown in Fig. 6 are $1^\circ \times 1^\circ$ averages (relative to the number of cloud free 5 km
315 CALIOP profiles in each $1^\circ \times 1^\circ$ regional bin) of $0.532 \mu\text{m}$ aerosol extinction coefficient
316 for the 0.0 to 0.5 km layer (Fig. 6a), 0.5-1.5 km (Fig. 6b), 1.5-2.5 km (Fig. 6c) and 2.5-
317 3.5 km a.g.l. (Fig. 6d), respectively. In general, extinction values observed in the lower
318 atmospheric layers (Figs. 6a and b) are larger than those observed in the elevated
319 atmospheric layers (Figs. 6c and d). However, higher mean values are found nearer the
320 surface in the eastern region (particularly the southeastern U.S.; Figs. 6a and b), while
321 higher values are found at elevated heights in the west (Figs. 6c and d). These data
322 indicate that, on average, aerosol particle distributions tend to be more concentrated near
323 the surface in the east and more diffuse vertically in the west.

324 Corresponding with Fig. 6a, Fig. 7 is a plot of the average percentage of surface
325 layer-integrated extinction (altitudes lower than 500 m a.g.l.) to total column AOD. We
326 use the average of the lower 500 m a.g.l. to represent the surface layer so as to minimize
327 ground flash contamination in the CALIOP data when observations are near the ground
328 [e.g., Campbell et al., 2012b]. Values are generally below 40% across the CONUS, with
329 higher values more concentrated in the eastern part of the country. The distribution is
330 noisy, however, and thus to better interpret these data, we present a five-year assessment

331 (2006-2011) of CALIOP data (Figure 8). Common patterns emerge, though more
332 distinctly, as higher percentages are again found over the east versus the west. In general,
333 however, AOD below 500 m a.g.l. accounts for only 30% or less of the total column
334 AOD across the U.S. This indicates that it is necessary to have a priori knowledge of the
335 ratio between near-surface integrated extinction to column-integrated AOD in order to
336 better characterize the likely representativeness of applying satellite AOD as a proxy for
337 surface $PM_{2.5}$ concentration.

338 Note that although integrated extinction over the lowest 500 m a.g.l. may not be
339 representative of the total column AOD, it is possible that the correlation between the two
340 could be high, and thus useful for satellite AOD/ $PM_{2.5}$ studies. Although not shown here,
341 we also compute the $1^\circ \times 1^\circ$ average correlation between integrated extinction from the
342 lowest 500 m a.g.l. and total column AOD. Globally over land, an average correlation
343 of 0.61 is found. For the United States, a similar value of 0.62 is calculated, with values
344 of 0.61 for the Eastern time zone and 0.57 for the Pacific. Importantly, the lack of
345 significant regional variability in these relationships indicates that although the Eastern
346 and Pacific time zones may exhibit different AOD surface contribution percentages,
347 integrated surface extinction correlates relatively consistently with total column AOD.
348 Still, given a perfect possible correlation of 1 between integrated surface level extinction
349 and $PM_{2.5}$ concentration, the correlation value of ~ 0.6 between the former with column-
350 integrated AOD might represent the best case scenario, on a regional average, that one
351 could derive presently for the satellite AOD to $PM_{2.5}$ concentration relationship. [This](#)
352 [agrees well with the findings reported in Hoff and Christopher \(2009\).](#)

353 To evaluate the influence of aerosol particle presence at elevated levels, in Fig. 9a

354 we show the fraction of CALIOP-retrieved column-integrated AOD found above an
355 arbitrary standard height of 2 km a.g.l., thus segregating mostly boundary layer particle
356 presence versus those propagating within the free troposphere. It is evident that regional
357 variations in the fraction of AOD above 2 km exist, as the western half of the U.S.
358 exhibits at least double the amount of particle extinction above 2 km than does the
359 eastern U.S. However, note that many areas in California, where a relatively dense array
360 of Pacific U.S. PM_{2.5} sites are located, exhibit relatively low contributions comparable to
361 that of the east (usually below 30%). Consistent with the findings shown in Fig. 9a,
362 regional variations in the frequency of occurrence of AOD above 2 km a.g.l. are also
363 observed (Fig. 9b), with generally higher frequencies in the west as compared to the east.

364 The average frequency of occurrence of aerosol particle presence (as measured by
365 CALIOP total column AOD) above 2 km a.g.l for the U.S. is ~ 40% (Fig. 9b). Also,
366 about 20% of data records (not shown) have at least 50% of aerosol particle presence
367 above 2 km a.g.l. This indicates a significant number of elevated aerosol plumes
368 occurred over the U.S. during the 2008-2009 period, and thus will not be recognized by
369 surface-based PM_{2.5} measurements.

370

371 **5.0 Can Near Surface Observations from CALIOP Be Used As a Better Proxy for** 372 **PM_{2.5} Concentration?**

373

374 Taking advantage of an active-profiling aerosol particle sensor like CALIOP, we
375 investigate the relationship between hourly PM_{2.5} concentration and CALIOP 532 μm
376 extinction coefficient values near the surface. The temporal/spatial collocation and 40
377 km AOD averaging process here is the same as described in Sec. 3. Recall that PM_{2.5} is a
378 dry particle mass measurement. However, satellite-retrieved AOD values include the

379 effects of aerosol particle growth as a function of vapor pressure. To compute the
380 CALIOP extinction and $PM_{2.5}$ relationship, a sensitivity study was performed for which
381 the hygroscopic growth of aerosol particles was accounted for. We approximate that
382 aerosol particles over the U.S. are sulfate aerosols, and apply the sulfate aerosol
383 hygroscopic growth factor [Hanel, 1976; Hegg et al., 1993; Anderson et al., 1994] to
384 compute dry aerosol extinction and AOD using Goddard Modeling and Assimilation
385 Office (GMAO) relative humidity values included as metadata in the NASA-
386 disseminated CALIOP files. No correction is made to extinction coefficient values when
387 relative humidity is less than 30% or above 95%. Further, we investigate the sensitivity
388 of the CALIOP value chosen to compare with by varying the height of the retrieval used
389 between 0 and 500 m a.g.l. in 100 m segments.

390 Results, including the level of CALIOP extinction used, are summarized in Table 5.
391 For both the Eastern and Pacific U.S. time zones, altering the level of the reported
392 CALIOP extinction from 200 to 500 m a.g.l. has little effect on correlation. Relatively
393 low correlation is observed using the CALIOP extinction values at the 0-100 m level,
394 however, suggesting the likely impacts of ground contamination of the backscatter signal.
395 When hygroscopic growth of aerosol particles is considered, modest improvements are
396 found for the Eastern U.S. but not the climatologically drier Pacific region.

397 We next investigate the relationship between CALIOP extinction near the surface
398 and $PM_{2.5}$ concentrations when collocated Aqua MODIS operational retrievals are
399 available. This $PM_{2.5}$ /CALIOP/Aqua MODIS dataset was constructed for both hourly
400 and daily analyses during the 2008-2009 period. For the hourly study, both CALIOP and
401 operational Aqua MODIS observations are again averaged within 40 km and the 1 hr of

402 the $PM_{2.5}$ measurements. For the daily comparison, observations from CALIOP are
403 averaged within 100 km along-track (approximately 1°), and those from operational Aqua
404 MODIS are averaged within 1° latitude/longitude, and the day of each $PM_{2.5}$
405 measurement.

406 Figure 10 shows hourly analysis results for dry mass-adjusted CALIOP extinction
407 at 200-300 m a.g.l. (Figure 10a) and operational Aqua MODIS AOD (Figure 10b). The
408 200-300 m layer was used because the lowest 200 m a.g.l. of retrieved extinction is
409 considered subject to ground contamination [e.g., Schuster et al., 2012; Omar et al., 2013].
410 Reasonably high correlations of ~ 0.8 are found for CALIOP/ $PM_{2.5}$ for both the Eastern
411 and Pacific time zones. A difference exists between these two regions for Aqua MODIS,
412 however. The Eastern U.S. exhibits similar correlation compared with that found above
413 from CALIOP, but drops off to about ~ 0.5 for the Pacific U.S. Clearly, CALIOP and
414 Aqua MODIS retrievals behave similarly for the Eastern U.S., but CALIOP performance
415 is much better than Aqua MODIS over the Pacific. However, the correlations between
416 $PM_{2.5}$ and CALIOP/Aqua MODIS observations computed in this analysis should be
417 considered with caution, as the low data count (fewer than 100 data points) make these
418 findings tenuous.

419 Figures 11a and b depict the same analyses as in Fig. 10, but now for the daily
420 analysis of $PM_{2.5}$ /CALIOP/Aqua MODIS. Correlations are reduced for each time zone,
421 compared with the hourly results. As was shown in Fig. 10, CALIOP and Aqua MODIS
422 exhibit similar correlations with daily $PM_{2.5}$ for the Eastern U.S., but daily
423 $PM_{2.5}$ /CALIOP correlations are better than daily $PM_{2.5}$ /Aqua MODIS correlations for the
424 Pacific U.S.

425 CALIOP near-surface extinction/ hourly $PM_{2.5}$ relationships represent the most
426 consistent correlations solved in this study. However, more research is necessary to
427 advance our understanding of the relationship between actively-profiled aerosol optical
428 properties and $PM_{2.5}$. This is particularly important since studies have reported
429 significant uncertainties in CALIOP AOD and extinction data [e.g., Schuster et al., 2012;
430 Omar et al., 2013], especially for values lower than 200 m a.g.l., which are clearly critical
431 to resolving the most optimal CALIOP extinction/ $PM_{2.5}$ relationship. Note, however, that
432 aside from ground contamination issues described above, Campbell et al., [2012a,b]
433 argue for an additional QA step of removing CALIOP profiles from bulk averages where
434 no aerosol extinction is retrieved below 200 m to limit the effects of signal pulse
435 attenuation. This effect may be further contributing to lower skill at these heights.
436 Further, additional analysis can be further explored where the top height of the surface-
437 detached mixed aerosol layer is known. This constraint was not considered here, and is
438 outside the general scope of our investigation.

439

440 **6.0 Conclusions**

441 Surface measurements of particulate matter with diameters less than $2.5 \mu m$ ($PM_{2.5}$)
442 are a frequent tool used to evaluate air quality in urban areas. Past studies have
443 investigated the ability of using aerosol optical depth (AOD) retrievals from passive
444 satellite sensors as proxies for $PM_{2.5}$ concentrations. Extending from past efforts, this
445 study explores the impact of passive satellite AOD data quality and satellite-derived
446 surface-to-column aerosol representativeness on the $PM_{2.5}$ /AOD relationship for a two-
447 year period (2008-2009). With a focus on the United States, passive AOD operational

448 Level-2 retrievals from Aqua/Terra Collection 5.1 Moderate Resolution Imaging
449 Spectroradiometer (MODIS) and Version 22 Multi-angle Imaging Spectroradiometer
450 (MISR) are temporally and spatially collocated for an hourly comparison with $PM_{2.5}$
451 measurements. Next, operational and data assimilation (DA) quality Aqua/Terra MODIS
452 and MISR AOD datasets are analyzed against $PM_{2.5}$ on a daily temporal scale to reveal
453 the effects that AOD data quality can exhibit with respect to $PM_{2.5}$ /AOD correlations.
454 The representativeness of surface aerosol particle concentration to that of the entire
455 column, as well as the correlation between surface AOD and total column AOD, are
456 investigated using observations from Cloud-Aerosol Lidar with Orthogonal Polarization
457 (CALIOP). CALIOP is then used to examine the relationship between near surface
458 aerosol extinction and $PM_{2.5}$.

459 The conclusions of this study are summarized as follows:

- 460 (1) Application of aggressive QA procedures to passive satellite AOD retrievals
461 increases their correlation with $PM_{2.5}$ for all of the CONUS, but significantly
462 decreases data counts by a factor of about 2.
- 463 (2) Correlations remain low even with aggressive QA.
- 464 (3) Aerosol particle distributions tend to be more concentrated near the surface in the
465 Eastern U.S and more diffuse vertically in the Western U.S. This regional
466 variability in aerosol vertical distribution across the CONUS confirms one reason
467 for the higher $PM_{2.5}$ /satellite AOD correlations observed in the east compared to
468 the west.
- 469 (4) Near-surface extinction (below 500 m a.g.l.), as measured by CALIOP, is not well
470 representative of total column-integrated extinction (i.e., AOD). Regionally,

471 near-surface aerosols are more representative of total column AOD in the Eastern
472 U.S. than in the Western U.S.

473 (5) Correlations between near-surface CALIOP 0.532 μm extinction and hourly $\text{PM}_{2.5}$
474 observations are better than can be achieved with passive AOD retrievals.
475 However, with fewer than 100 pairs of collocated $\text{PM}_{2.5}$ and CALIOP extinction
476 data points used, such a finding is tenuous. Additional studies are needed to
477 further explore the possibility of accurately estimating $\text{PM}_{2.5}$ concentrations from
478 surface extinction derived from active sensors.

479
480 In this paper, we have demonstrated that estimation of $\text{PM}_{2.5}$ concentrations from
481 satellite retrieved AOD is limited by both the quality of satellite AOD retrievals as well
482 as the representativeness of column-integrated AOD to near surface AOD. Also, some of
483 the past studies have shown that passive satellite AOD may be used to accurately
484 estimate $\text{PM}_{2.5}$ for particular sites. However, this study shows that, even with the use of
485 higher-quality DA AOD observations, column-integrated AOD derived from passive
486 satellite sensors may not be used directly as accurate proxies for surface-based $\text{PM}_{2.5}$ over
487 broad spatial domains. As discussed earlier, this is partly attributed to differences in the
488 aerosol surface-to-column representativeness across the CONUS. Therefore, we caution
489 the direct use of passive satellite AOD observations for $\text{PM}_{2.5}$ estimation over large areas,
490 especially in regions where elevated aerosol plumes exist.

491 Additionally, as our initial study has shown, the use of near surface extinction
492 measurements from active sensors, such as CALIOP, may provide a better $\text{PM}_{2.5}$
493 estimation over broad spatial scales than column-integrated passive satellite AOD.

494 However, ground contamination for near-surface CALIOP measurements and the effects
495 of humidity on aerosol optical properties need further investigation. Still, satellite
496 derived aerosol properties are of much value to PM_{2.5} studies, especially with the
497 synergistic use of passive and active aerosol-sensitive observations, and through
498 assimilating these quality-assured data into air-quality focused numerical models for
499 future PM_{2.5} monitoring and forecasts.

500

501

502

503

504 **ACKNOWLEDGEMENTS**

505 This research was funded through the support of the Office of Naval Research Code 322
506 and the NASA Interdisciplinary Science Program. Author JRC acknowledges the support
507 of NASA Interagency Agreement NNG13HH10I on behalf of the Micropulse Lidar
508 Network and NASA Radiation Sciences Program. Author YS acknowledges the support
509 of the NASA Earth and Space Science Fellowship (NESSF) Program. CALIPSO and
510 MISR data were obtained from the NASA Langley Research Center Atmospheric
511 Science Data Center. MODIS data were obtained from NASA Goddard Space Flight
512 Center. The DA-quality MODIS data were obtained from the Global Ocean Data
513 Assimilation Experiment (GODAE) server.

514

515 **REFERENCES**

516

517 Anderson, T. L., Charlson, R. J., White, W. H., and McMurry, P. H.: Comment on “Light
518 scattering and cloud condensation nucleus activity of sulfate aerosol measured over
519 the Northeast Atlantic Ocean” by D.A. Hegg et al., *J. Geophys. Res.*, 99(D12),
520 25947–25949, doi:10.1029/94JD02608, 1994.

- 521
522 Anderson, T. L., Charlson, R. J., Winker, D. M., Ogren, J. A., and Holmén, K.:
523 Mesoscale variations of tropospheric aerosols, *J. Atmos. Sci.*, 60, 119–136, 2003b.
524
- 525 Boyouk, N., Léon, J. F., Delbarre, H., Podvin, T., and Deroo, C.: Impact of the mixing
526 boundary layer on the relationship between PM_{2.5} and aerosol optical
527 thickness. *Atmospheric Environment*, 44(2), 271-277, 2010.
528
- 529 Campbell, J. R., Tackett, J. L., Reid, J. S., Zhang, J., Curtis, C. A., Hyer, E. J., Sessions,
530 W. R., Westphal, D. L., Prospero, J. M., Welton, E. J., Omar, A. H., Vaughan, M. A.,
531 and Winker, D. M.: Evaluating nighttime CALIOP 0.532 μm aerosol optical depth
532 and extinction coefficient retrievals, *Atmos. Meas. Tech.*, 5, 2143–2160,
533 doi:10.5194/amt-5-2143-2012, 2012a.
534
- 535 Campbell, J. R., Reid, J. S., Westphal, D. L., Zhang, J., Tackett, J. L., Chew, B. N.,
536 Welton, E. J., Shimizu, A., Sugimoto, N., Aoki, K., and Winker, D. M.:
537 Characterizing the vertical profile of aerosol particle extinction and linear
538 depolarization over southeast Asia and the maritime continent: the 2007–2009 view
539 from CALIOP, *Atmos. Res.*, 122, 520–543, doi:10.1016/j.atmosres.2012.05.007,
540 2012b.
541
- 542 Chu, D. A., Kaufman, Y. J., Zibordi, G., Chern, J. D., Mao, J., Li, C., and Holben, B N.:
543 Global monitoring of air pollution over land from the Earth Observing System-Terra
544 Moderate Resolution Imaging Spectroradiometer (MODIS), *J. Geophys. Res.*, 108,
545 4661, doi:10.1029/2002JD003179,D21, 2003.
546
- 547 Diner, D. J., Beckert, J. C., Reilly, T. H., Bruegge, C. J., Conel, J. E., Kahn, R. A.,
548 Martonchik, J. V., Ackerman, T. P., Davies, R., Gerstl, S. A. W., Gordon, H. R.,
549 Muller, J.-P., Myneni, R. B., Sellers, P. J., Pinty, B., and Verstraete, M. M.: Multi-
550 angle Imaging SpectroRadiometer (MISR) instrument description and experiment
551 overview, *IEEE Trans. Geosci. Remote Sens.*, 36, 1072–1087, 1998.
552
- 553 Engel-Cox, J. A., Hoff, R. M., Rogers, R., Dimmick, F., Rush, A. C., Szykman, J., Al-
554 Saadi, J., Chu, D. A., and Zell, E. R.: Integrating lidar and satellite optical depth with
555 ambient monitoring for 3-dimensional particulate characterization. *Atmos. Environ.*,
556 40, 8056–8067, 2006.
557
- 558 Engel-Cox, J. A., Holloman, C. H., Coutant, B. W., and Hoff, R. M.: Qualitative and
559 quantitative evaluation of MODIS satellite sensor data for regional and urban scale air
560 quality. *Atmos. Environ.*, 38, 2495–2509, 2004.
561
- 562 Federal Register: National ambient air quality standards for particulate matter. Final Rule
563 Federal Register/vol. 62, no. 138/Friday, July 18, 1997/Final Rule, 40 CFR Part 50,
564 1997.
565
- 566 Federal Register: National ambient air quality standards for particulate matter. Proposed

- 567 Rule Federal Register/vol. 71, no. 10/Tuesday, January 17, 2006/Proposed Rules, 40
568 CFR Part 50, 2006.
- 569
- 570 Gupta, P., Christopher, S.A., Wang, J., Gehrig, R., Lee, Y.C., and Kumar, N.: Satellite
571 remote sensing of particulate matter and air quality over global cities. *Atmospheric*
572 *Environment* 40 (30), 5880–5892, 2006.
- 573
- 574 Hanel, G.: The properties of atmospheric aerosol particles as functions of relative
575 humidity at thermodynamic equilibrium with surrounding moist air, *Adv. Geophys.*,
576 19, 73–188, 1976.
- 577
- 578 Hegg, D. A., Ferek, R. J., and Hobbs, P. V.: Light scattering and cloud condensation
579 nucleus activity of sulfate aerosol measured over the northeast Atlantic Ocean, *J.*
580 *Geophys. Res.*, 98(D8), 14887–14894, doi:10.1029/93JD01615, 1993.
- 581
- 582 Hoff, R. M. and Christopher, S. A.: Remote sensing of particulate pollution from space:
583 have we reached the promised land?, *J Air Waste Manag Assoc.*, 59:645–675, 2009.
- 584
- 585 [Holben, B.N., Eck, T.F., Slutsker, I., Tanré, D., Buis, J.P., Setzer, A., Vermote, E.,](#)
586 [Reagan, J. A., Kaufman, Y., Nakajima, T., Lavenu, F., Jankowiak, I., and Smirnov,](#)
587 [A.: AERONET - A federated instrument network and data archive for aerosol](#)
588 [characterization, *Rem. Sens. Environ.*, 66, 1-16, 1998.](#)
- 589
- 590 Hu, Z.: Spatial analysis of MODIS aerosol optical depth, PM_{2.5}, and chronic coronary
591 heart disease, *Int. J. Health Geogr.*, 8, 27, doi:10.1186/1476-072X-8-27, 2009.
- 592
- 593 Hunt, W. H., Winker, D. M., Vaughan, M. A., Powell, K. A., Lucker, P. L., and Weimer,
594 C.: CALIPSO lidar description and performance assessment, *J. Atmos. Oceanic*
595 *Technol.*, 26, 1214–1228, doi:10.1175/2009JTECHA1223.1, 2009.
- 596
- 597 Hutchison, K. D.: Applications of MODIS satellite data and products for monitoring air
598 quality in the state of Texas. *Atmos. Environ.*, 37, 2403–2412, 2003.
- 599
- 600 Hyer, E. J. and Chew, B. N.: Aerosol transport model evaluation of an extreme smoke
601 episode in Southeast Asia, *Atmos. Environ.*, 44(11), 1422–1427, 2010.
- 602
- 603 Hyer, E. J., Reid, J. S., and Zhang, J.: An over-land aerosol optical depth data set for data
604 assimilation by filtering, correction, and aggregation of MODIS Collection 5 optical
605 depth retrievals, *Atmos. Meas. Tech.*, 4, 379–408, doi:10.5194/amt-4-379-2011, 2011.
- 606
- 607 Kahn, R. A., Gaitley, B. J., Martonchik, J. V., Diner, D. J., Crean, K. A., and Holben,
608 B. N.: Multiangle Imaging Spectroradiometer (MISR) global aerosol optical depth
609 validation based on 2 years of coincident Aerosol Robotic Network (AERONET)
610 observations, *J. Geophys. Res.*, 110, D10S04, doi:10.1029/2004JD004706, 2005.
- 611
- 612 Kahn, R. A., Gaitley, B. J., Garay, M. J., Diner, D. J., Eck, T., Smirnov, A. and

- 613 Holben, B. N.: Multiangle Imaging Spectroradiometer global aerosol product
614 assessment by comparison with Aerosol Robotic Network, *J. Geophys. Res.*, 115,
615 D23209, doi:10.1029/2010JD014601, 2010.
- 616
617 Kittaka, C., Winker, D. M., Vaughan, M. A., Omar, A., and Remer, L. A.:
618 Intercomparison of column aerosol optical depths from CALIPSO and MODIS-Aqua,
619 *Atmos. Meas. Tech.*, 4, 131–141, doi:10.5194/amt-4-131-2011, 2011.
- 620
621 Kumar, N., Chu, A., and Foster, A.: An empirical relationship between PM_{2.5} and
622 aerosol optical depth in Delhi Metropolitan, *Atmos. Environ.*, 41, 4492–4503, 2007.
- 623
624 Liu, Y., Park, R. J., Jacob, D. J., Li, Q., Kilaru, V., and Sarnat, J. A.: Mapping annual
625 mean ground-level PM_{2.5} concentrations using Multiangle Imaging
626 Spectroradiometer aerosol optical thickness over the contiguous United States, *J.*
627 *Geophys. Res.*, 109, D22206, doi:10.1029/2004JD005025, 2004.
- 628
629 Liu, Y., Franklin, M., Kahn, R., and Koutrakis, P.: Using aerosol optical thickness to
630 predict ground-level PM_{2.5} concentrations in the St Louis area: a comparison
631 between MISR and MODIS. *Remote Sens Environ* 107:33–44, 2007.
- 632
633 Omar, A. H., Winker, D. M., Tackett, J. L., Giles, D. M., Kar, J., Liu, Z., Vaughan, M. A.,
634 Powell, K. A., and Trepte, C. R.: CALIOP and AERONET aerosol optical depth
635 comparisons: One size fits none, *J. Geophys. Res. Atmos.*, 118, 4748–4766,
636 doi:10.1002/jgrd.50330, 2013.
- 637 Paciorek, C., Liu, Y., Moreno-Macias, H., and Kondragunta, S.: Spatio-temporal
638 associations between GOES aerosol optical depth retrievals and ground-level PM_{2.5}.
639 *Environ Sci Technol* 42:5800–5806, 2008.
- 640
641 Pope III., C. A., Burnett, R. T., Thun, M. J., Calle, E. E., Krewski, D., Ito, K., and
642 Thurston, G.D.: Lung cancer, cardiopulmonary mortality, and long-term exposure to
643 fine particulate air pollution. *Journal of the American Medical Association* 287,
644 1132–1141, 2002.
- 645
646 Prados, A. I., Kondragunta, S., Ciren, P., and Knapp, K. R.: GOES Aerosol/Smoke
647 Product (GASP) over North America: Comparisons to AERONET and MODIS
648 observations, *J. Geophys. Res.*, 112, D15201, doi:10.1029/2006JD007968, 2007.
- 649
650 Remer, L. A., Kaufman, Y. J., Tanre, D., Mattoo, S., Chu, D. A., Martins, J. V., Li, R.-R.,
651 Ichoku, C., Levy, R. C., Kleidman, R. G., Eck, T. F., Vermote, E., and Holben, B. N.:
652 The MODIS aerosol algorithm, products, and validation, *J. Atmos. Sci.*, 62, 947–973,
653 2005.
- 654
655 Schuster, G. L., Vaughan, M., MacDonnell, D., Su, W., Winker, D., Dubovik, O.,
656 Lapyonok, T., and Trepte, C.: Comparison of CALIPSO aerosol optical depth
657 retrievals to AERONET measurements, and a climatology for the lidar ratio of
658 dust, *Atmos. Chem. Phys. Discuss.*, 12, 11641–11697, 2012.

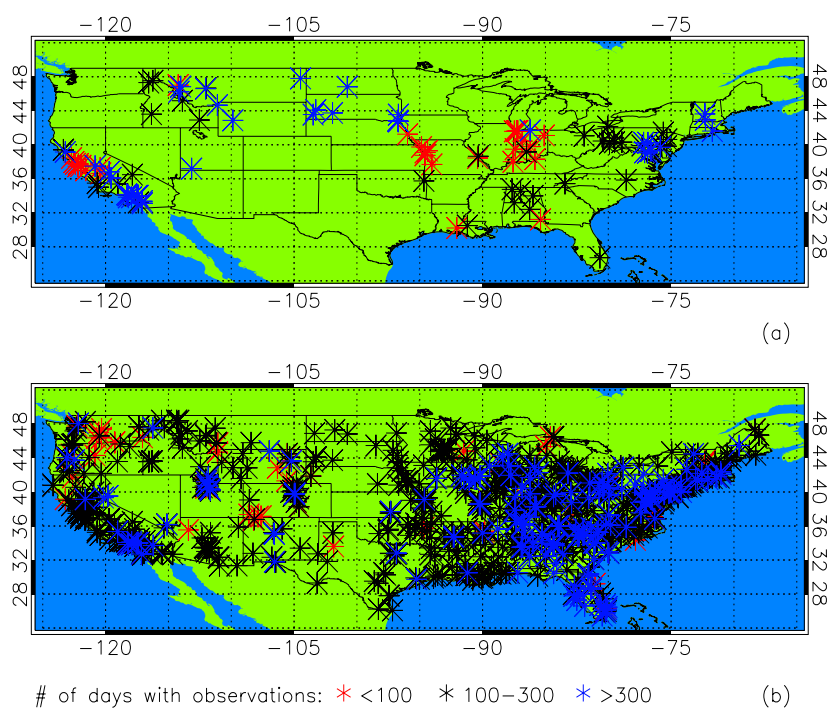
- 659
660 Schwartz, J., and Neas, L. M.: Fine particles are more strongly associated than coarse
661 particles with acute respiratory health effects in school children. *Epidemiology*, 11,
662 6–10, 2000.
- 663
664 Shi, Y., Zhang, J., Reid, J. S., Holben, B., Hyer, E. J., and Curtis, C.: An analysis of the
665 Collection 5 MODIS over-ocean aerosol optical depth product for its implication in
666 aerosol assimilation, *Atmos. Chem. Phys.*, 11, 557–565, doi:10.5194/acp-11-557-
667 2011a, 2011.
- 668
669 Shi, Y., Zhang, J., Reid, J. S., Liu, B., and Deshmukh, R.: Multi-sensor Analysis on Data-
670 Assimilation-Quality MISR Aerosol Products, Abstract A53C-0358 presented at 2011
671 Fall Meeting, AGU, San Francisco, Calif., 5-9 Dec, 2011b.
- 672
673 Shi Y., Zhang, J., Reid, J. S., Liu, B., and Deshmukh, R.: Critical evaluation of cloud
674 contamination in MISR aerosol product using collocated MODIS aerosol and cloud
675 products, Abstract A13J-0310, presented at 2012 Fall Meeting, AGU, San Francisco,
676 Calif., 3-7 Dec, 2012.
- 677
678 Shinozuka, Y., Clarke, A. D., Howell, S.G., Kapustin, V. N., McNaughton, C. S., Zhou,
679 J., and Anderson, B. E.: Aircraft profiles of aerosol microphysics and optical
680 properties over North America: Aerosol optical depth and its association with PM_{2.5}
681 and water uptake, *J. Geophys. Res.*, 112, D12S20, doi:10.1029/2006JD007918, 2007.
- 682
683 Stephens, G. L., Vane, D. G., Boain, R. J., Mace, G. G., Sassen, K., Wang, Z.,
684 Illingworth, A. J., O'Connor, E. J., Rossow, W. B., Durden, S. L., Miller, S. D.,
685 Austin, R. T., Benedetti, A., and Mitrescu, C.: The CloudSat mission and the A-Train:
686 A new dimension of space-based observations of clouds and precipitation. *Bull. Amer.*
687 *Meteorol. Soc.*, 83, 1771–1790, doi:10.1175/BAMS-83-12-1771, 2002.
- 688
689 Toth, T. D., Zhang, J., Campbell, J. R., Reid, J. S., Shi, Y., Johnson, R. S., Smirnov, A.,
690 Vaughan, M. A., and Winker, D. M.: Investigating enhanced Aqua MODIS aerosol
691 optical depth retrievals over the mid-to-high latitude Southern Oceans through
692 intercomparison with co-located CALIOP, MAN, and AERONET data sets, *J.*
693 *Geophys. Res. Atmos.*, 118, 4700-4714, doi:10.1002/jgrd.50311, 2013.
- 694
695 van Donkelaar, A., Martin, R. V., and Park, R. J.: Estimating ground-level PM_{2.5} using
696 aerosol optical depth determined from satellite remote sensing. *Journal of*
697 *Geophysical Research* 111, D21201, doi:10.1029/2005JD006996, 2006.
- 698
699 van Donkelaar A., Martin, R. V., Brauer, M., Kahn, R., Levy, R., Verduzco, C., and
700 Villeneuve, P. J.: Global estimates of ambient fine particulate matter concentrations
701 from satellite-based aerosol optical depth: development and application. *Environ*
702 *Health Perspect*, 118:847–855, 2010.
- 703
704 Wang, J., and Christopher, S. A.: Intercomparison between satellite derived aerosol

705 optical thickness and PM2.5 mass: implications for air quality studies. *Geophysical*
706 *Research Letters* 30 (21), 2095, doi:10.1029/2003GL018174, 2003.
707
708 Winker, D. M., Hunt, W. H., and McGill, M. J.: Initial performance assessment of
709 CALIOP, *Geophys. Res. Lett.*, 34, L19803, doi:10.1029/2007GL030135, 2007.
710
711 Winker, D. M., Tackett, J. L., Getzewich, B. J., Liu, Z., Vaughan, M. A., and Rogers, R.
712 R.: The global 3-D distribution of tropospheric aerosols as characterized by CALIOP.
713 *ACPD*, doi:10.5194/acpd-12-1-2012, 2012.
714
715 Zhang, J., Christopher, S. A., and Holben, B. N.: Intercomparison of smoke aerosol
716 optical thickness derived from GOES 8 imager and ground-based Sun photometers, *J.*
717 *Geophys. Res.*, 106, D7, doi: 10.1029/2000JD900540, 2001.
718
719 Zhang, J., and Reid, J. S.: MODIS aerosol product analysis for data assimilation:
720 Assessment of over-ocean level 2aerosol optical thickness retrievals, *J. Geophys. Res.*,
721 111, D22207, doi:10.1029/2005JD006898, 2006.
722
723 Zhang, J., Reid, J. S., Westphal, D. L., Baker, N. L., and Hyer, E. J.: A system for
724 operational aerosol optical depth data assimilation over global oceans, *J. Geophys.*
725 *Res.*, 113, D10208, doi:10.1029/2007JD009065, 2008.
726
727 Zhang, J., Campbell, J. R., Reid, J. S., Westphal, D. L., Baker, N. L., Campbell, W. F.,
728 and Hyer, E. J.: Evaluating the impact of assimilating CALIOP-derived aerosol
729 extinction profiles on a global mass transport model, *Geophys. Res. Lett.*, 38, L14801,
730 doi:10.1029/2011GL047737, 2011.
731
732
733
734
735
736
737
738
739
740
741
742
743
744
745
746
747
748
749
750

751 | **FIGURES**

752

753



754

755

756

757 | **Figure 1**

758

759 | For 2008-2009, U.S. Environmental Protection Agency (EPA) sites with available $PM_{2.5}$

760 | measurements at (a) hourly and (b) daily intervals, respectively. The sites are colored-

761 | coded based on number of days with observations, as red (fewer than 100), black

762 | (between 100 and 300), or blue (greater than 300).

763

764

765

766

767

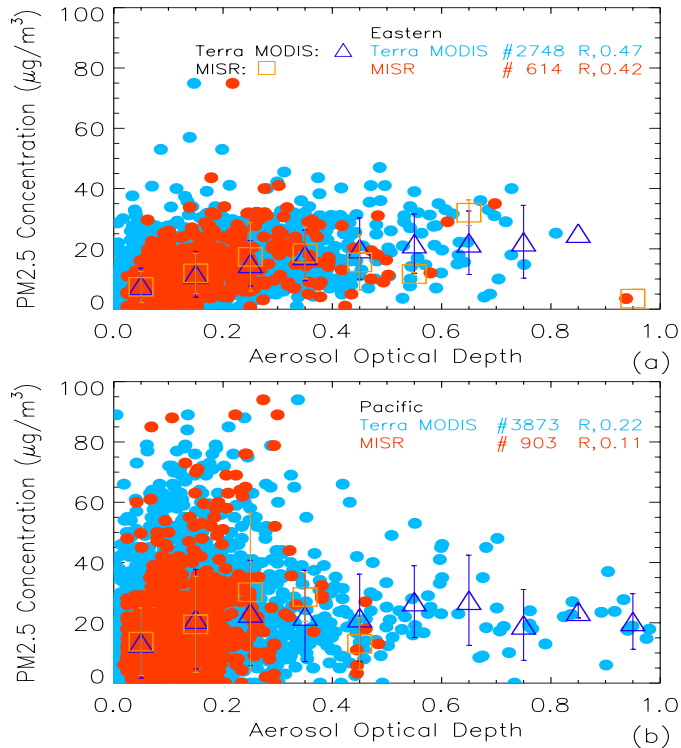
768

769

770

771

772



773

774

775 **Figure 2**

776

777 Two-year (2008-2009) scatterplots of operational Terra MODIS (in light blue) and MISR

778 (in red) AOD, averaged within 40 km of each respective PM_{2.5}-monitoring site, versus779 hourly PM_{2.5} concentrations for the (a) Eastern and (b) Pacific U.S. time zones. Also780 plotted are averages of PM_{2.5} for each 0.1 AOD bin, represented with triangles (in dark

781 blue) for Terra MODIS and squares (in orange) for MISR. Error bars (+/- 1 standard

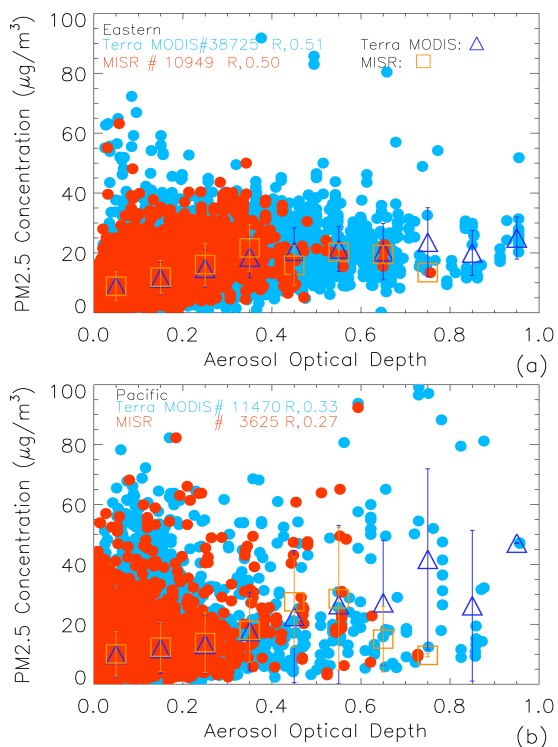
782 deviation) for the bin averages are also shown.

783

784

785

786



787

788

789 **Figure 3**

790

791 Two-year (2008-2009) scatterplots of daily $1^\circ \times 1^\circ$ DA Terra MODIS (in light blue) and792 daily $1^\circ \times 1^\circ$ MISR (in red) AOD versus daily $PM_{2.5}$ concentrations for the (a) Eastern793 and (b) Pacific U.S. time zones. Averages of $PM_{2.5}$ are plotted for each 0.1 AOD bin,

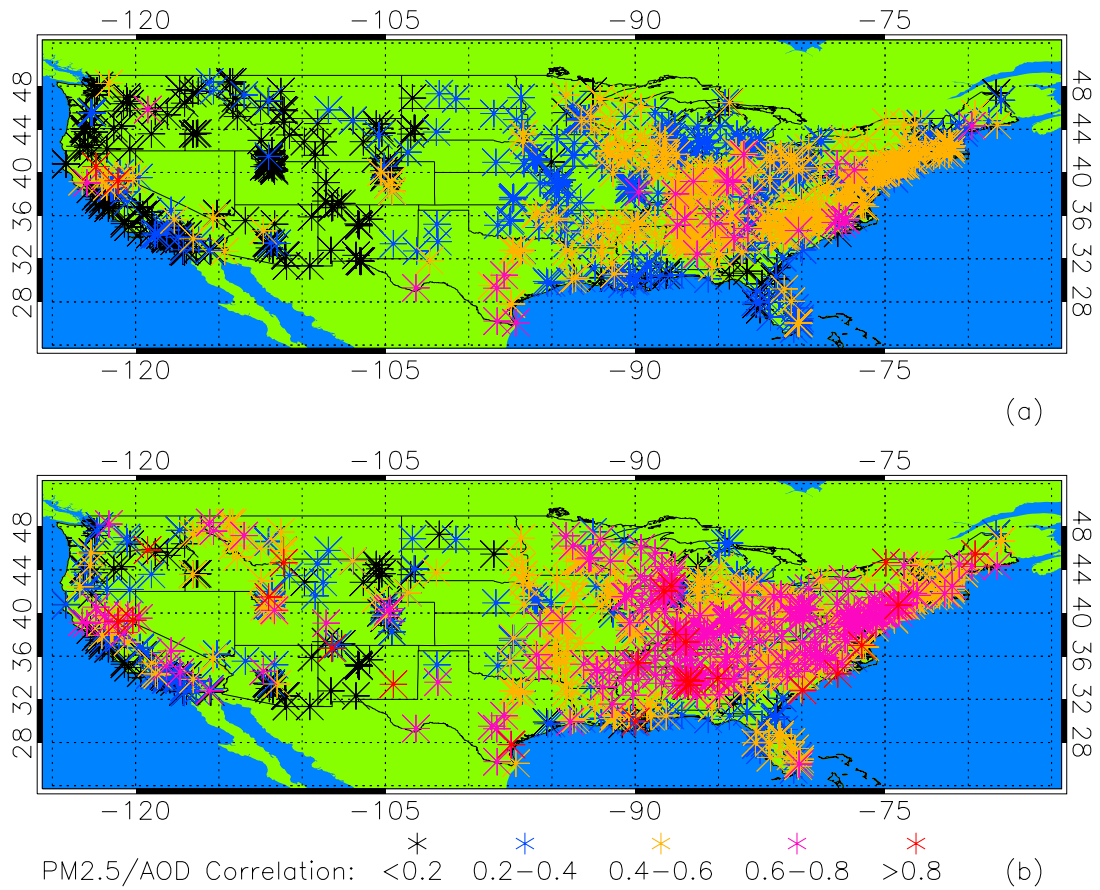
794 represented with triangles (in dark blue) for Terra MODIS and squares (in orange) for

795 MISR. Error bars (± 1 standard deviation) for the bin averages are also shown.

796

797

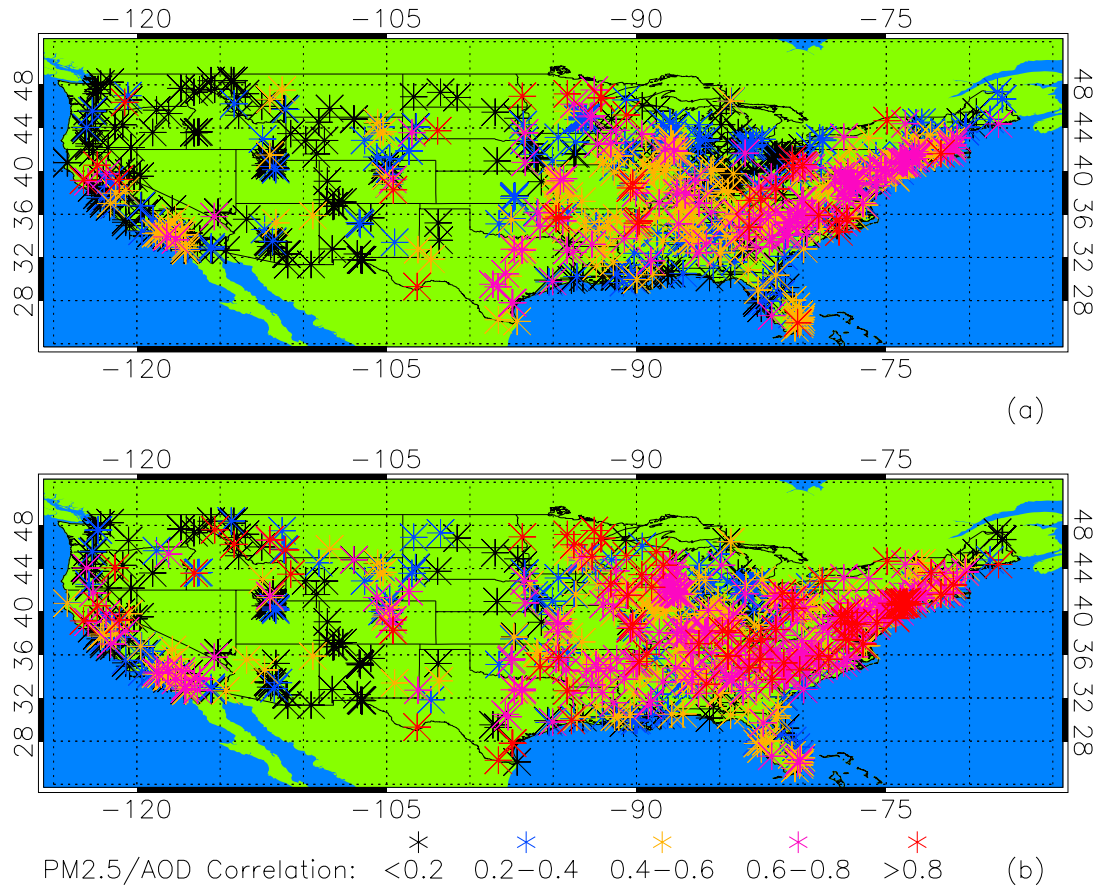
798



799
800
801
802
803
804
805
806
807
808
809
810
811
812
813
814

Figure 4

For 2008-2009, those U.S. Environmental Protection Agency (EPA) daily PM_{2.5} sites used in this study. Sites are color-coded based on the correlation between daily PM_{2.5} observations and daily 1° x 1° (a) operational and (b) DA Terra MODIS AOD.



815

816 **Figure 5**

817

818 For 2008-2009, U.S. Environmental Protection Agency (EPA) daily PM_{2.5} sites used in819 this study. Sites are color-coded based on the correlation between daily PM_{2.5}

820 observations and daily 1° x 1° (a) operational and (b) DA MISR AOD.

821

822

823

824

825

826

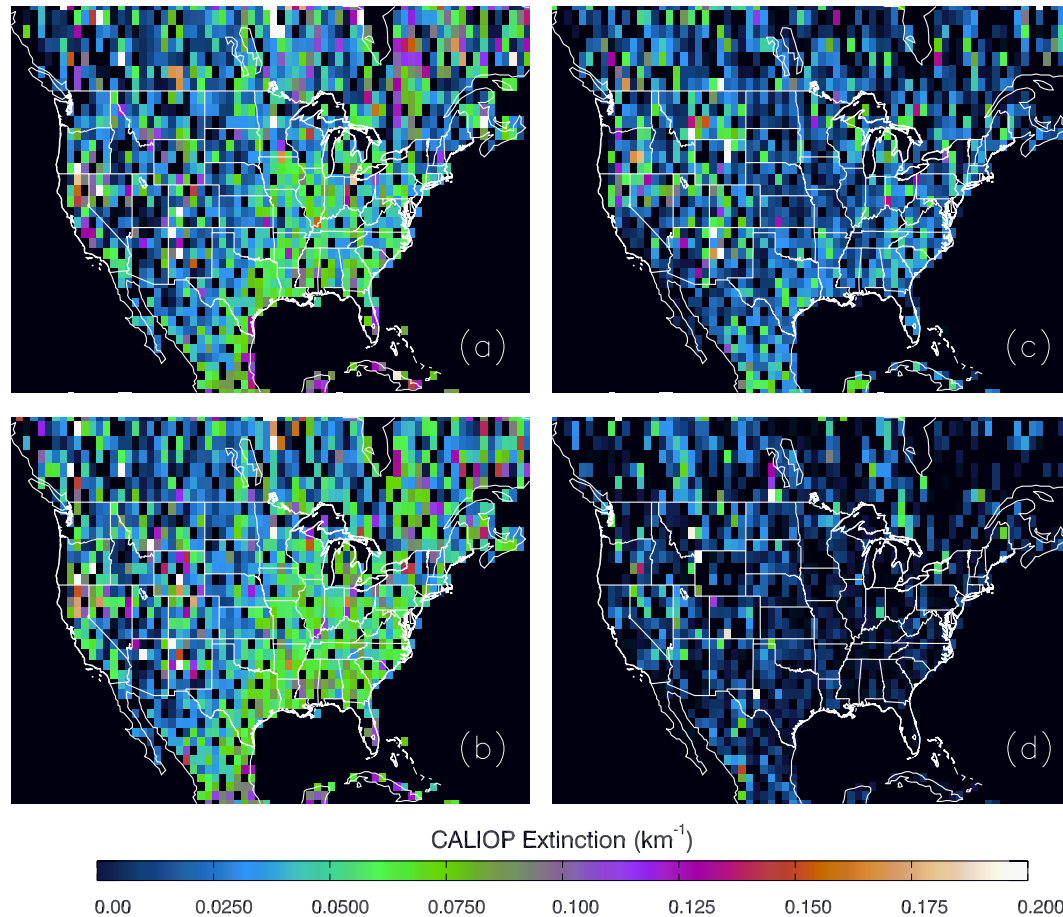
827

828

829

830

831



832

833

834 **Figure 6**

835

836 Two-year (2008-2009) 1° x 1° average CALIOP 0.532 μm extinction, relative to the

837 number of cloud free 5 km CALIOP profiles in each 1° x 1° bin, for atmospheric layers

838 a.g.l. of (a) 0-500 m, (b) 500-1500 m, (c) 1500-2500 m, and (d) 2500-3500 m.

839

840

841

842

843

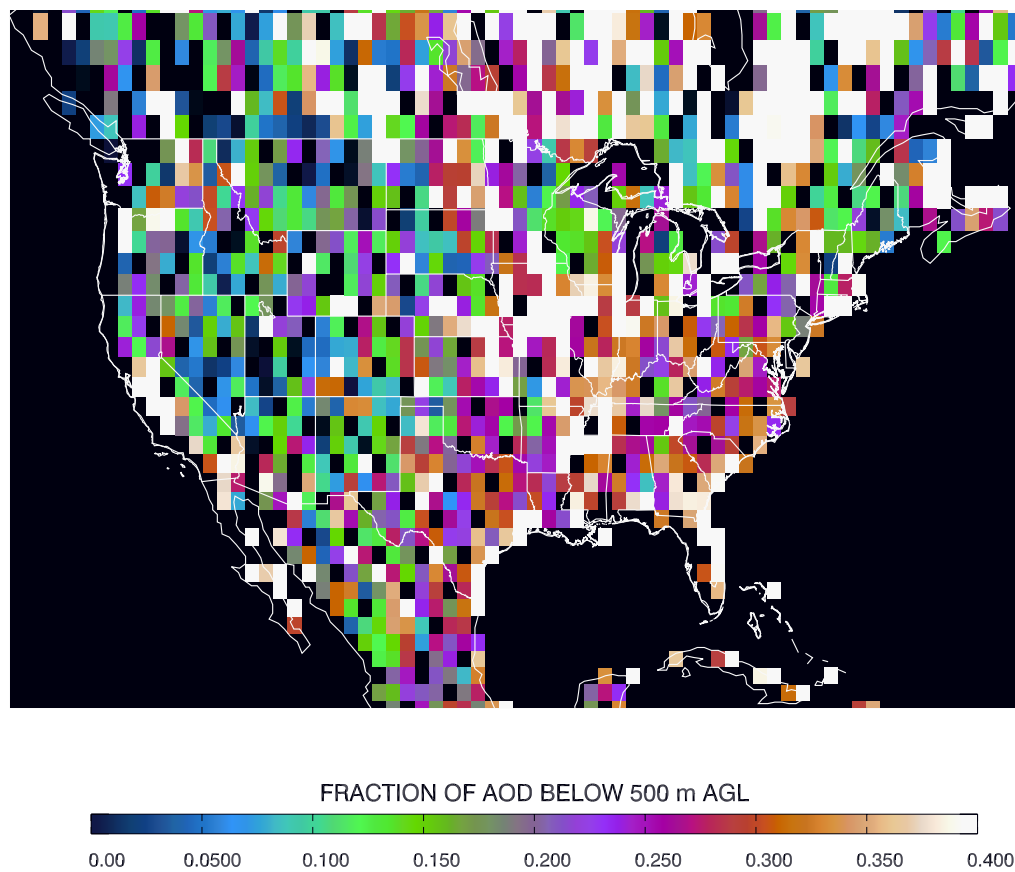
844

845

846

847

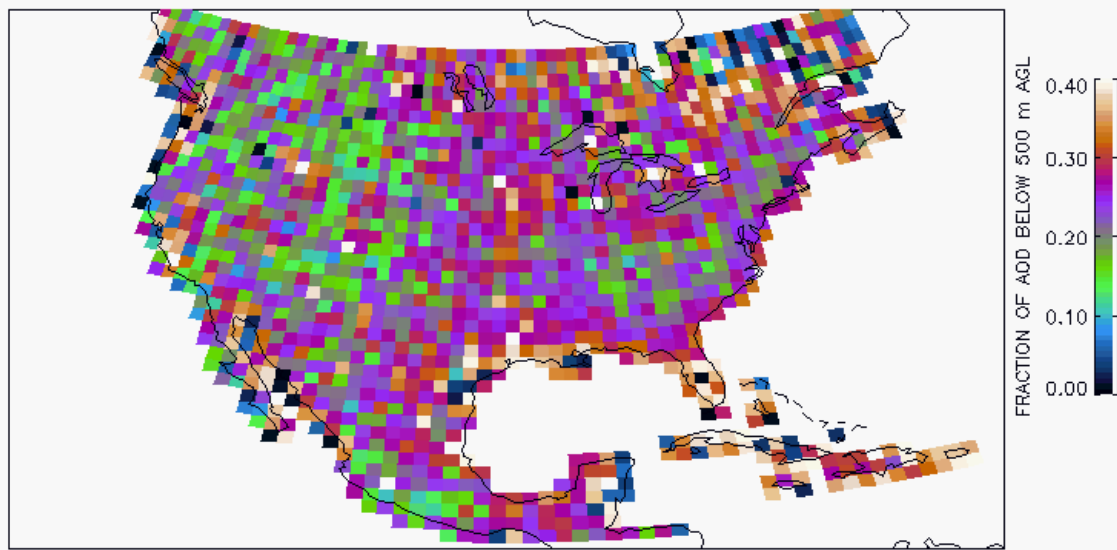
848
849
850



851
852
853
854
855
856
857

Figure 7

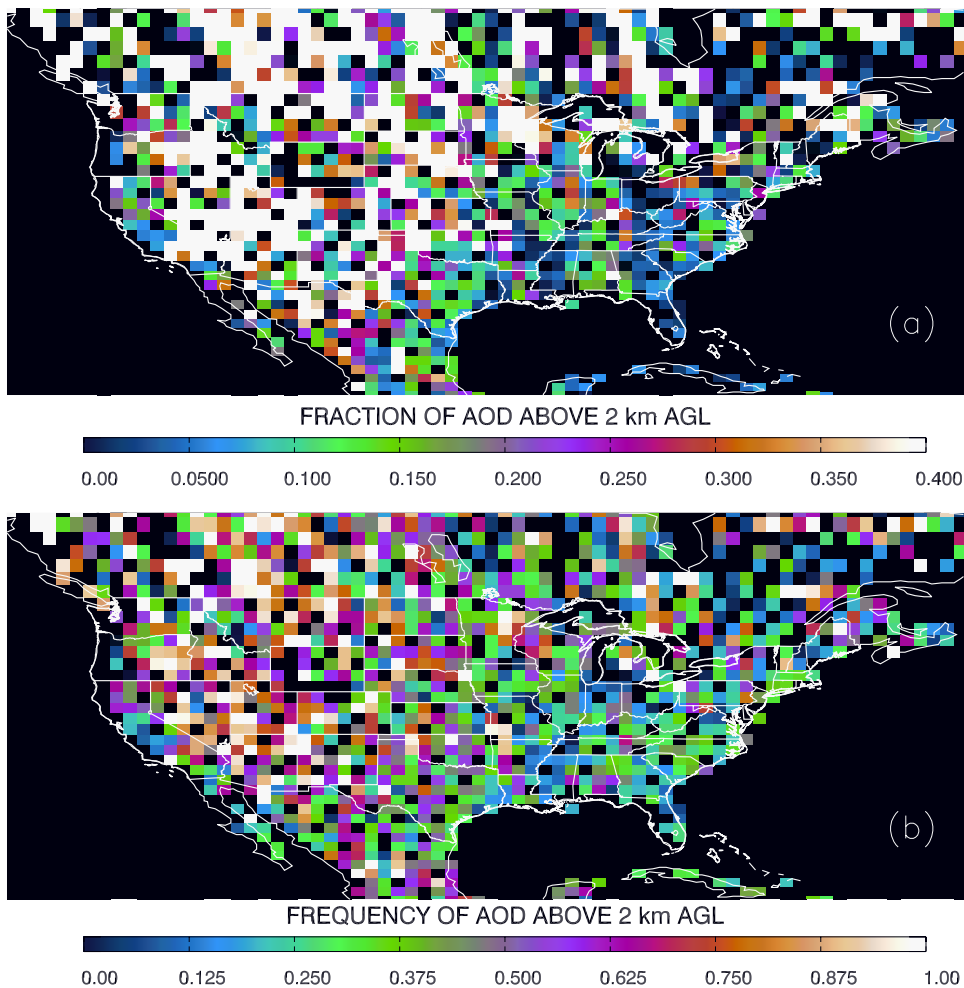
Two-year (2008-2009) 1° x 1° average contribution percentage of 0 to 500 m a.g.l. integrated CALIOP extinction to total column AOD (at 0.532 μm) relative to the number of cloud free CALIOP profiles in each 1° x 1° bin, for the Continental United States.



858
859
860
861
862
863
864
865
866
867
868
869
870
871
872
873
874
875
876
877
878
879
880
881
882
883
884
885
886
887

Figure 8

From 2006-2011, fraction of CALIOP integrated 0.532 μm extinction below 500 m a.g.l. for the Continental United States.



888

889 **Figure 9**

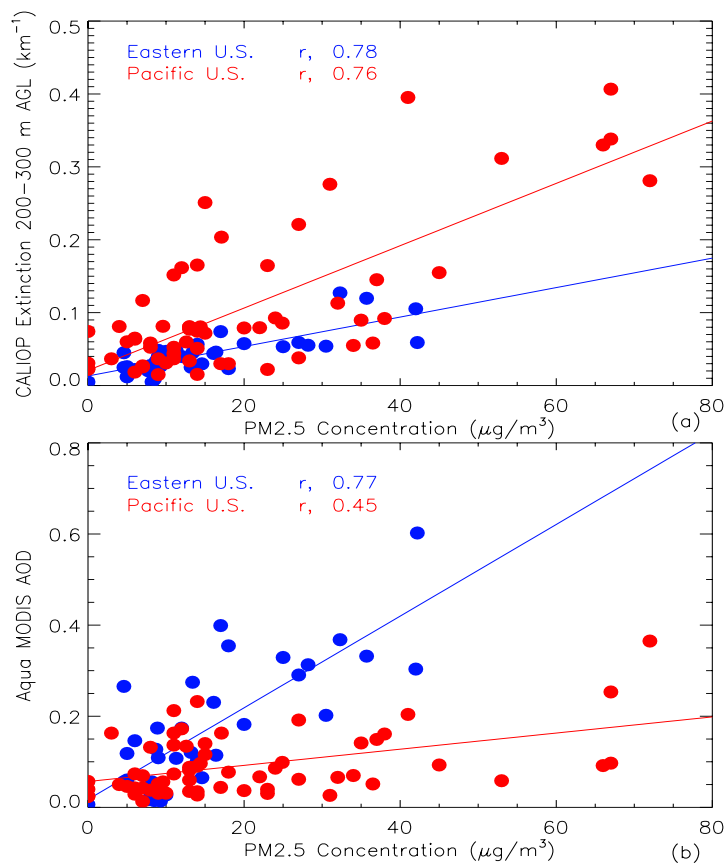
890

891 Two-year (2008-2009) $1^\circ \times 1^\circ$ average (a) contribution percentage of above 2 km a.g.l.892 CALIOP AOD to total column AOD (at $0.532 \mu\text{m}$) and (b) frequency of occurrence of

893 AOD above 2 km a.g.l., both relative to the number of cloud-free CALIOP profiles in

894 each $1^\circ \times 1^\circ$ bin, for the Continental United States.

895



896

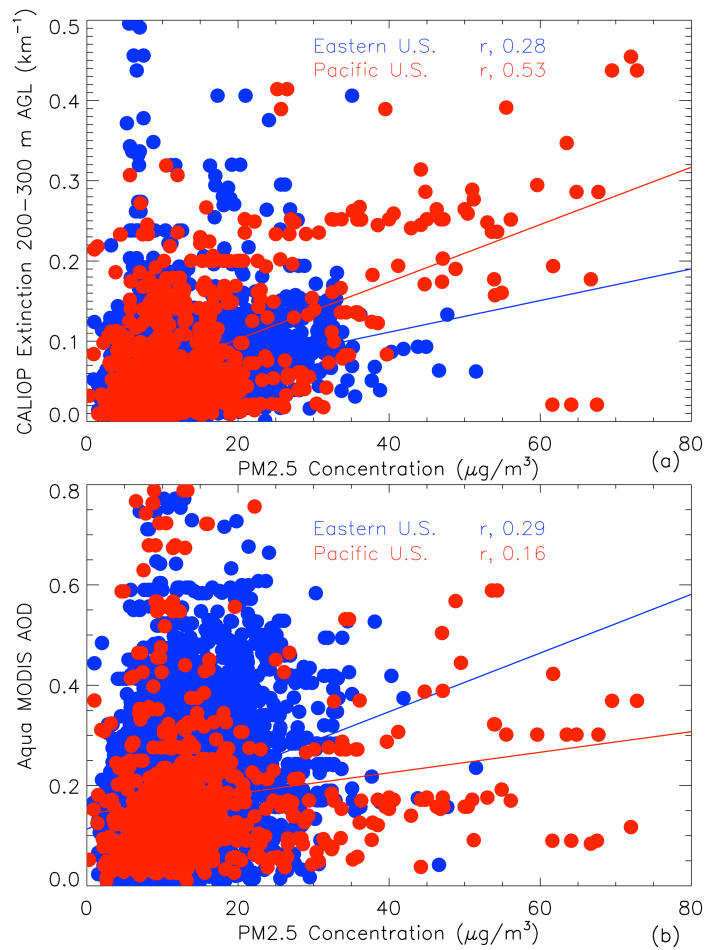
897

Figure 10

898

899 For the Eastern (in blue) and Pacific (in red) U.S. Time zones, two-year (2008-2009)

900 scatterplots of hourly PM_{2.5} concentrations versus (a) cloud-free 5 km CALIOP dry mass901 0.532 μm extinction at the 200-300 m a.g.l. layer, and (b) operational Aqua MODIS902 AOD, both averaged within 40 km and the hour of each respective PM_{2.5} measurement.



903

904 **Figure 11**

905 For the Eastern (blue) and Pacific (red) U.S. Time zones, two-year (2008-2009)

906 scatterplots of daily PM_{2.5} concentrations versus (a) cloud-free 5 km CALIOP dry mass

907 0.532 μm extinction at the 200-300 m a.g.l. layer (averaged within 100 km), and (b)

908 operational Aqua MODIS AOD (averaged within 1°) and the day of each respective

909 PM_{2.5} measurement.

910

911

912 **TABLES**

913

Dataset		Operational Aqua MODIS		Operational Terra MODIS		Operational MISR	
		R value	Data Count	R value	Data count	R value	Data count
Eastern	All	0.57	2081	0.47	2748	0.42	614
	DJFMAM	0.49	477	0.39	566	0.11	154
	JJASON	0.57	1551	0.50	2001	0.50	408
Central	All	0.27	1765	0.22	2005	0.22	447
	DJFMAM	0.11	335	0.14	346	0.16	112
	JJASON	0.38	1330	0.28	1511	0.26	304
Mountain	All	0.19	1369	0.12	1632	0.10	391
	DJFMAM	-0.08	215	0.09	250	0.16	95
	JJASON	0.30	1136	0.17	1354	0.20	277
Pacific	All	0.15	3832	0.22	3873	0.11	903
	DJFMAM	0.08	1064	0.21	1047	0.15	269
	JJASON	0.26	2560	0.21	2564	0.29	539
Contiguous U.S.	All	0.19	9047	0.22	10258	0.15	2355
	DJFMAM	0.03	2091	0.12	2209	0.07	630
	JJASON	0.34	6577	0.25	7430	0.27	1528

914

915 **Table 1**

916

917 Correlation coefficients and data counts of the 40 km average operational Aqua/Terra

918 MODIS and MISR AOD/hourly PM_{2.5} collocation analyses for the Eastern, Central,

919 Mountain, and Pacific time zones and continental United States total for the entire two-

920 year (2008-2009) study period, December through May 2008-2009 (DJFMAM), and June

921 through November 2008-2009 (JJASON).

922

923

924

925

926

927

928

929

930

931

Dataset		Aqua MODIS				Terra MODIS				MISR			
		Operational		DA		Operational		DA		Operational		DA	
		R value	Data Count	R value	Data Count	R value	Data Count	R value	Data Count	R value	Data Count	R value	Data Count
Eastern	All	0.40	76194	0.50	29682	0.38	80810	0.51	38725	0.32	15526	0.50	10949
	DJFMAM	0.23	30615	0.31	12180	0.23	32492	0.35	15166	0.20	6819	0.37	4829
	JJASON	0.45	43837	0.56	17123	0.44	45839	0.55	22723	0.37	8194	0.55	5750
Central	All	0.39	39942	0.47	18584	0.36	40824	0.51	21084	0.30	8396	0.46	6256
	DJFMAM	0.27	15892	0.31	7507	0.22	15853	0.29	8130	0.23	3536	0.35	2549
	JJASON	0.45	23217	0.55	10708	0.44	23979	0.57	12506	0.33	4649	0.53	3551
Mountain	All	0.09	14160	0.21	5007	0.07	15597	0.13	6313	0.04	3455	0.06	2489
	DJFMAM	0.06	4788	0.00	1180	0.04	5258	-0.04	1463	-0.01	1385	-0.05	782
	JJASON	0.13	9178	0.30	3775	0.13	10078	0.29	4793	0.12	1974	0.16	1659
Pacific	All	0.13	21871	0.33	11446	0.12	22405	0.33	11470	0.16	4639	0.27	3625
	DJFMAM	0.00	9110	0.08	4218	-0.03	9308	0.08	4265	0.06	2047	0.16	1509
	JJASON	0.24	12310	0.44	7107	0.24	12470	0.43	7011	0.27	2431	0.37	2025
Contiguous U.S.	All	0.31	152167	0.43	64719	0.29	159636	0.45	77592	0.26	32016	0.40	23319
	DJFMAM	0.15	60405	0.21	25085	0.12	62911	0.22	29024	0.15	13787	0.26	9669
	JJASON	0.40	88542	0.52	38713	0.39	92366	0.52	47033	0.34	17248	0.48	12985

932
933
934
935
936
937
938
939

Table 2

Correlation coefficients and data counts of the daily 1° x 1° average operational/DA Aqua/Terra MODIS and MISR AOD/daily PM_{2.5} collocation analyses for the Eastern, Central, Mountain, and Pacific time zones and continental United States total for the entire two-year (2008-2009) study period, December through May 2008-2009 (DJFMAM), and June through November 2008-2009 (JJASON).

940
941
942
943

Dataset	Aqua MODIS			Terra MODIS			MISR		
	Hourly R value	Daily R value	Data Count	Hourly R value	Daily R value	Data Count	Hourly R value	Daily R value	Data Count
Eastern	0.63	0.54	369	0.52	0.58	543	0.56	0.49	138
Central	0.29	0.2	305	0.25	0.28	362	0.20	0.12	93
Mountain	0.52	0.56	108	0.35	0.55	119	0.39	-0.08	21
Pacific	0.32	0.16	916	0.25	0.21	874	0.25	0.15	270
Contiguous US	0.36	0.20	1698	0.30	0.25	1898	0.30	0.22	522

944
945
946
947
948
949
950
951
952
953
954
955

Table 3

Correlation coefficients and data counts for the hourly $PM_{2.5}/40$ km average operational AOD and daily $PM_{2.5}/1^\circ \times 1^\circ$ average DA AOD common point analyses for the Eastern, Central, Mountain, and Pacific time zones and continental United States total for the two-year (2008-2009) study period.

Dataset	R value	Data Count
Eastern	0.57	6596
Central	0.39	613
Mountain	0.12	2438
Pacific	0.47	512
Contiguous US	0.47	10159

956
957
958
959
960
961
962
963

Table 4

Correlation coefficients and data counts for the hourly PM_{2.5}/average AERONET AOD (0.670 μm) collocation analysis (AERONET AOD averaged within the hour and 0.3° latitude/longitude of an hourly PM_{2.5} measurement) for the Eastern, Central, Mountain, and Pacific time zones and continental United States total for the two-year (2008-2009) study period.

964

CALIOP Extinction Layer	Uncorrected CALIOP Extinction		Dry Mass CALIOP Extinction	
	Eastern	Pacific	Eastern	Pacific
0 - 100 m	0.35	0.72	0.33	0.71
100 - 200 m	0.62	0.73	0.66	0.72
200 - 300 m	0.57	0.72	0.69	0.74
300 - 400 m	0.54	0.61	0.63	0.59
400 - 500 m	0.69	0.58	0.70	0.56

965

966

967 | **Table 5**

968

969 Two-year (2008-2009) correlation coefficients of hourly PM_{2.5} observations and 40 km average CALIOP extinction (both uncorrected

970 and dry mass) at various 100 m a.g.l. atmospheric layers.

971

972

973

974

975

976

977

978